

Torrefaction of olive mill waste

Verónica Benavente*, Andrés Fullana

Chemical Engineering Department, University of Alicante, Ap. 99, E-03080 Alicante, Spain

**Corresponding author. E-mail: veronica.benavente@ua.es. Tlf.: +(34) 965 90 34 00 ext. 1116.*

Fax: +(34) 965 90 38 26.

Abstract

Two-phase olive mill waste (TPOMW) was converted via torrefaction into a carbon rich solid interesting as bioenergy feedstock. TPOMW was characterized and torrefied in an oven at temperatures ranging from 150 to 300 °C for 2 hours. Mass and energy losses occurred during torrefaction were measured and the torrefied products were characterized including ultimate analysis, heating value measurements, accelerate solvent extraction (ASE) and FTIR in order to assess the effects of torrefaction on the physicochemical properties of TPOMW. Additionally, ash fouling evaluation was also performed through XRF analysis. The weight fraction of C, defined in percentage as wt.%, improved from 56 to 68 wt.% and the high heating value rose from 26.4 to 30.0 MJ•kg⁻¹ as torrefaction temperature increased, reaching typical values of subbituminous coal and finding the best results at 200 °C in terms of maximizing the heating value and minimizing the energy losses. Accordingly, from FTIR analysis it was observed that the degree of coalification increased during torrefaction of TPOMW. ASE results shown that the residual olive oil in TPOMW was removed during torrefaction, being completely eliminated at 300 °C. The alkali index for TPOMW was

25 found to be 0.66 kg alkali•GJ-1, which implied a high fouling tendency that could be
26 mitigated through co-firing. Finally, t-TPOMW briquettes with good mechanical
27 strength and energy density of 26.7 GJ•m⁻³ were produced using a hydraulic piston
28 press. Results demonstrated that torrefaction allows transforming TPOMW into a coal-
29 like material, which would imply a profitable way to manage these wastes.

30

31 **Keywords:** Torrefaction, biomass, upgrading, olive mill waste, densification, bioenergy.

32

33 **1. Introduction**

34 Motivated by the transition to a more sustainable society based on clean energy
35 technologies, biomass emerges as one of the most important renewable energy sources,
36 on the one hand, due to its environmental benefits, since bioenergy could imply a
37 reduction in the carbon dioxide emissions and contributes to decrease the environmental
38 impact caused by organic wastes, on the other, because it constitutes a key factor in the
39 economic development of rural areas and enhances energy access [1, 2]. Over the past
40 decade, the bioenergy utilization increased from 8% of the world total primary energy
41 supply to 10% today and it is expected to rise further to between 25% and 33% by 2050
42 [1]. However, an important transition required to achieve this vision is to use biomass
43 more efficiently by deploying more efficient conversion technologies and better
44 integrating bioenergy production into biomass value chains in other industries.

45

46 There is a considerable bioenergy potential from several sources, since a wide range of
47 feedstocks can be used for bioenergy generation, like energy crops, biomass residues
48 and organic wastes. In the northern European countries, is common to refer to wood

49 biomass (e.g. bark, wood chips and sawdust). Nevertheless, the Mediterranean area has
50 great bioenergy potential from several agricultural residues, especially from the olive oil
51 sector as they produce over 98% of the worldwide production [3].

52

53 The olive-oil extraction process generates large amounts of byproducts and wastes that
54 require a specific management regarding minimization, valorization and mitigation of
55 their environmental impact. The new technology for olive-oil extraction is a continuous
56 centrifugate two-phase process that generates a liquid phase (olive oil) and an organic
57 slurry called two-phase olive mill waste (TPOMW, or ‘alperujo’ in Spanish). In Spain
58 (major olive oil producer country), alone this new system generates approximately
59 300000 tons per year of TPOMW [4], which is a high polluting by-product due to its
60 content in organic matter. Indeed, the pollutant power of TPOMW is very high (BOD
61 $89\text{-}100\text{ g}\cdot\text{L}^{-1}$, COD $80\text{-}200\text{ g}\cdot\text{L}^{-1}$, being BOD and COD the Biological Oxygen Demand
62 and the Chemical Oxygen Demand, respectively) as the TPOMW organic fraction
63 includes sugars, polyalcohols, pectins, lipids and notable amounts of aromatic
64 compounds that are responsible for phytotoxic and antimicrobial effects [5, 6].
65 Nowadays, there is not an efficient elimination system of TPOMW due to its low
66 energy density and its high moisture content, which makes it costly to transport, in
67 combination with other technological limitations as low combustion efficiency [7].
68 Thus, it is imperative to find a proper disposal or utilization of viable management
69 strategies.

70

71 Torrefaction is a mild pyrolysis process that can help to overcome some of the above
72 mentioned limitations by converting biomass into an upgraded solid material with

73 increased energy density and decreased oxygen content, therefore more suitable for
74 energy generation. This method comprises thermal treating of material at temperatures
75 from 200 to 300°C so that neither great initial investment nor high operating costs are
76 required [7-9].

77

78 The torrefaction products are volatile (carbon dioxide, carbon monoxide and possible
79 traces of acetic acid, hydrogen and methane), condensable and non-condensable gases
80 (water vapor, acetic acid, furfural, formic acid, methanol, lactic acid, phenol), and a
81 carbon-enriched solid, which is the main torrefaction product, that retains between 75
82 and 95% from the departure energy content, depending on the processing conditions
83 (pressure, temperature, residence time) and the feedstock [9]. Wannapeera and
84 Worasuwanarak [10] studied the torrefaction under pressure of leucaena and found that
85 the mass and energy yield was higher when raising the torrefaction pressure. Other
86 authors [7, 11-15] examined the influence of torrefaction temperature and residence
87 time on the properties of torrefied materials obtained from different feedstocks and
88 observed that, although both parameters affect the product distribution and the
89 properties of the solid, the temperature had more effect on torrefaction than the
90 residence time. Pimchuai et al. [7] study the torrefaction in nitrogen atmosphere of rice
91 husks, sawdust, peanut husks, bagasse and water hyacinth at temperatures ranging from
92 250 °C to 300 °, and found that the combustion properties of the torrefied materials were
93 improved for the higher torrefaction temperatures investigated. Chen et al. [12]
94 investigate the torrefaction behavior of lauan blocks and recommended the operation at
95 250 °C and 1 h in order to intensify the heating value as well as to avoid too much mass
96 loss of the initial wood and its conversion into condensed liquid. On the other hand,

97 Rousset et al. [16] evaluated the combined effect of the temperature and oxygen
98 concentrations on the physical and chemical properties of eucalyptus grandis and from
99 the results it was possible to confirm that the oxygen concentration become important
100 on the properties and compositions of the solid from over 280 °C, being negligible at
101 lower temperatures.

102

103 The torrefied material is comparable with a low rank coal and still retains some
104 characteristic properties from the original biomass but present higher energy content
105 and better stability against microbial degradation due to the improved hydrophobic
106 properties. Besides, torrefied biomass is a fragile and low density porous product that
107 has a higher dust formation capacity and lower mechanical strength than fresh biomass
108 due to the loss of structural integrity from the breakdown of hemicellulose [9].

109 Consequently, these characteristics make it necessary to volumetrically densify the
110 torrefied material in order to facilitate its handling and reducing transport and storage
111 costs.

112

113 Among the variety of densification systems, pellet mill and briquette press are the most
114 common technologies used for producing a uniform format feedstock product for
115 bioenergy applications [17]. Studies of torrefied biomass densification have indicate
116 that the pressure and the energy required during the briquetting process are reduced by a
117 factor of two while the performance increases twice as compared to the densification
118 process of fresh biomass [17]. Hence, torrefaction combined with briquetting or
119 pelletizing could be an efficient option for treating agricultural wastes and produce
120 bioenergy feedstock.

121

122 Despite torrefaction of diverse biomass resources can be found in the literature [12-14,
123 18-21], there is still a gap of information in the implementation of this technique as an
124 efficient management treatment to minimize and valorize problematic organic wastes,
125 such as the TPOMW. In this work, the torrefaction method has been applied to
126 TPOMW in order to study the viability of the process to produce bioenergy feedstock
127 from the olive oil extraction waste. Different experiments were carried out at laboratory
128 scale in order to determinate the optimum temperature of the process. Then, the
129 torrefied materials were fully characterized in order to evaluate its potential as a biofuel.
130 Finally, briquetting tests were performed to test the applicability of this technique to the
131 torrefied TPOMW (t-TPOMW).

132

133 **2. Materials and Methods**

134

135 *2.1. Materials*

136 Fresh TPOMW was supplied by Extremadura Agricultural and Food Technological
137 Centre (CTAEX) during the olive campaign for 2012-2013. This material was sun dried
138 on the field for two weeks. Then, the residual moisture content was obtained from the
139 total mass loss after drying the fresh TPOMW in an oven at 105 °C for 24 h, which was
140 found to be 5.8 wt.%. The dried TPOMW material was milled in a grinder to attain
141 homogeneity, since the olive pits were easy to detect among the dried pulp, sieved to
142 obtain a particle size less than 0.5 mm (particle size distribution between 0.1 and 0.5
143 mm) and characterized including ultimate analysis, ash content, heating value tests and
144 thermal analysis. Results are summarized in Table 1.

145

146 *2.2. Torrefaction experiment procedure*

147 Several tests were proposed to investigate the effect of the temperature on the TPOMW
148 torrefaction process. To accomplish this, TPOMW was torrefied under different
149 temperature conditions in an oven model UFP500 from Memmert GmbH with an
150 internal volume of 108 L. Experiments were carried out at 150, 200, 250 and 300 °C for
151 2 hours and the mass loss was registered at the end. Temperatures 150 °C and 200 °C
152 were included in the studied torrefaction temperature range in order to analyze if any
153 change happened to the olive oil retained in the waste and if it could have any effect on
154 the solid product since the smoke point of the olive oil is 160°C. In each experiment,
155 100 g of TPOMW were extended on a flat rectangular metal pan forming a thin layer.
156 When the oven reached the operating temperature, the metal pan was introduced in it.
157 After the specified residence time period, the metal pan was removed from the oven and
158 the solid product was weight and cooled until room temperature. Then, it was stored in
159 plastic sealed buckets for the subsequent characterization.

160

161 The torrefied samples (t-TPOMW-150, t-TPOMW-200, t-TPOMW-250, t-TPOMW-
162 300) were characterized through elemental analysis CHNS and heating value tests in
163 order to compare their properties with the ones of the raw material (TPOMW).

164

165 *2.3. Analytical methods*

166

167 *2.3.1. Ultimate analysis, ash fouling evaluation*

168 A CHNS analysis for dried TPOMW and for each t-TPOMW sample was carried out in
169 an Elemental CHNS Microanalyzer Thermo Finningan Flash 1112 Series. The ash
170 content of dried TPOMW was determined by thermal treating of TPOMW in a Muffle
171 serie-74 model 12-R/300 from Heron at 550 °C during 8 hours under atmospheric
172 condition. Oxygen content was calculated by subtraction of the ash and the CHNS
173 content from the total. It should be noted that the ash content for t-TPOMW samples
174 was recalculated from the content found for TPOMW by considering the mass loss
175 occurred during torrefaction. In addition, X-ray fluorescence (XRF) analysis was used
176 to determine the ash composition in order to assess the ash fusibility. A Philips
177 Analytical MagiX-PRO X-ray Fluorescence Spectrometer (XRF) was used to determine
178 the ash compositions in terms of weight fractions of the main oxide constituents.

179

180 *2.3.2. Heating value measurement*

181 Heating values of dried TPOMW and t-TPOMW were measured using an AC-350
182 Oxygen Bomb Calorimeter from Leco Corporation, which had an integral water-
183 measuring and combustion vessel-filling station. The equipment was calibrated using
184 benzoic acid and the measurement was performed at least by duplicate for each sample.
185 About 1 g of sample was loaded into the apparatus and combusted at 25 °C under a
186 pressure of 3 MPa of pure oxygen.

187

188 *2.3.3. Thermogravimetric analysis (TGA)*

189 A Perkin Elmer Pyris TGA/STA 6000 Thermogravimetric Analyzer was used to check
190 the thermal stability of dried TPOMW both in inert atmosphere. The sample mass was

191 around 5 mg and the heating program consisted on a 1 min hold at 35 °C and ramp up to
192 600°C at 20°C·min⁻¹ under nitrogen flow of 20 mL·min⁻¹.

193

194 *2.3.4. Accelerate solvent extraction (ASE)*

195 All the samples were subjected to accelerated extraction with hexane in order to
196 determine the residual content of olive oil. For this purpose, a DionexTM ASETM 150
197 Accelerated Solvent Extractor equipment was employed under the following conditions:
198 10 MPa, 100 °C, static time of 5 minutes, 3 static cycles, 70% flush and a purge time of
199 120 s. After extraction, the content of the pre-weighed extraction vials were evaporated
200 to dryness and the weight of the residue obtained was used to calculate the amount of
201 olive oil in the original samples.

202

203 *2.3.5. FTIR spectroscopy*

204 FTIR analyses of TPOMW and t-TPOMW were performed with a BRUKER IFS 66/S
205 instrument using pellets of potassium bromide that was previously oven-dried to reduce
206 interferences from water. Additionally, an olive oil sample was also examined by
207 depositing a small quantity between two well-polished KBr disks to create a thin film.
208 Each spectrum was recorded in the wavenumber range from 4000 to 600 cm⁻¹ with a
209 resolution of 2 cm⁻¹.

210

211 *2.4. Briquetting tests*

212 Finally, a hydraulic piston press fitted with an electrical oven was used to produce t-
213 TPOMW briquettes. Compression cell allows the production of a 5 cm diameter
214 briquette. The procedure consisted of making two successive compressions and

215 decompressions at 200 °C under 17 MPa, and subsequently cooling to room temperature
216 while maintaining the pressure, being the briquette finally demolded. Then, the
217 briquettes were extracted in the ASE equipment under the same conditions than before
218 (see point 2.3.4.) in order to determine the percentage of residual olive oil removed
219 from the torrefied material during the briquetting tests.

220

221 **3. Results and Discussion**

222

223 *3.1. Torrefaction of TPOMW*

224

225 *3.1.1. Characteristics of TPOMW and t-TPOMW*

226 Figure 1 shows the appearance of the torrefied materials derived at the various
227 temperatures. Visually, it was found that the appearance of the samples evolved from a
228 brown lignocellulosic to black coal-like as the torrefaction process was more severe.

229

230 Table 1 shows the ultimate analysis, the residual olive oil content and the high heating
231 value (HHV) for the raw and torrefied materials (TPOMW and t-TPOMW). It is noted
232 that the weight fraction of carbon, defined in percentage as wt.%, increases from 56 to
233 68 wt.% with the increase in the torrefaction temperature due to the elimination of
234 oxygen and hydrogen [9]. The HHV is higher than 28 MJ·kg⁻¹ (dry basis) for t-
235 TPOMW-200, t-TPOMW-250 and t-TPOMW-300. Thus, the HHV of the torrefied
236 products increases between 8.6 and 13.4% for the samples obtained at torrefaction
237 temperatures equal to or above 200 °C, being the HHV rise defined as HHV rise =
238 $((\text{HHV}_T - \text{HHV}_0) / \text{HHV}_0) \cdot 100$, where the HHV_T is the high heating value of the torrefied

239 sample obtained at temperature T and HHV_0 is the high heating value of raw TPOMW.
240 Comparing this result with the literature, it is observed that the rise in the HHV contents
241 are lower than those found for other torrefied agricultural residues, such as rice hulks,
242 sawdust, peanut husks, bagasse and water hyacinth [7], whose HHV rises reach values
243 over 20% at 300°C. However, the HHV of TPOMW is higher than those for the
244 aforementioned residues, and consequently, the torrefied TPOMW samples are more
245 energetic than the torrefied products obtained from the feedstocks mentioned before,
246 reaching typical values of subbituminous coal [22].

247

248 Figure 2.a presents the CHO diagram, which illustrates the effect of torrefaction
249 temperature on the ultimate analysis of the torrefied material obtained. Weight fractions
250 of C, H and O are normalized as $wt.\%C + wt.\%H + wt.\%O = 100$ for each t-TPOMW
251 sample. In addition, the CHO composition of carbon dioxide, carbon monoxide, water
252 vapor and acetic acid is also included in Figure 2.a, as they are expected to be the main
253 volatile and non-condensable products in torrefaction [8, 9, 23]. In that sense, the CHO
254 composition of oleic acid is represented as well.

255

256 It is observed that the C, H and O wt.% depends on the thermal treating temperature. C
257 wt.% increases as the temperature does, while the O wt.% decreases and H wt.%
258 remains almost constant until 250 °C, from which temperature it slightly decreases.

259 Furthermore, a mass balance over the ternary diagram was done. It is observed that, as
260 temperature increases, the t-TPOMW composition linearly moves in the opposite
261 direction to the area over which the carbon dioxide, carbon monoxide, vapor water and
262 acetic acid are situated. This observation suggests that, on the one hand, these

263 components could have been released during the torrefaction process as constituents of
264 the gas product flow, in agreement with the literature [9], and, on the other hand, that
265 they were released in higher quantities as the temperature increased, as expected, due to
266 a higher extent of the reactions involved during the torrefaction process. Accordingly, it
267 could be said in rough outlines that at temperatures below 250 °C the major reaction
268 pathways would have been decarboxylation reactions to form carbon monoxide, carbon
269 dioxide and solid torrefied TPOMW while at higher temperatures dehydration and
270 deacetylation reactions would also have become important. At 300 °C, t-TPOMW also
271 moves in the opposite direction over which oleic acid (main component of olive oil) is
272 placed, which suggests that the residual olive oil that still remained in the TPOMW was
273 removed during torrefaction.

274

275 In Table 1 is shown the olive oil content determined through ASE analysis. It is seen
276 that residual olive oil was removed during torrefaction, being completely eliminated at
277 300 °C, as predicted from the results observed in elemental analysis. Therefore, from
278 these results it could be concluded that torrefaction improves the properties of TPOMW
279 as a bioenergy feedstock, not only because enhance the carbon content and its heating
280 value but also because depending on torrefaction temperature, decreases or even entirely
281 removes the residual olive oil content, thus preventing from possible odors.

282

283 It is known that olive oil is composed mainly of mixed triglyceride esters of oleic acid
284 and palmitic acid and of other fatty acids, which decompose before vaporization. Font
285 and Rey [24] carried out a kinetic study of olive oil pyrolysis by thermogravimetry and
286 determined that the decomposition of the olive oil occurs in the temperature range of

287 230- 480 °C under the scheme of two consecutive reactions. The first global reaction
288 takes place between 280 and 450 °C and represents a process with decomposition
289 reactions and vaporization of the products obtained, whereas the second global reaction
290 takes place between 380 and 480 °C and involved complex decomposition reactions of
291 the products obtained in reaction 1. Consequently, the residual olive oil was removed
292 from the solid by means of decomposition reactions and volatilization of the products
293 formed during torrefaction.

294

295 t-TPOMW samples are also situated on the van Krevelen diagram (Fig. 2.b), where the
296 transition from the biomass composition to the corresponding coal is indicated. By this
297 figure, it is intended to illustrate that torrefaction allows transforming the TPOMW into
298 a material with characteristics similar to those of carbon, showing again the fall of the
299 H/C ratio against to that corresponding to oleic acid at temperatures higher than 200°C.
300

301 *3.1.2. Termogravimetric análisis*

302 Figure 3 shows the TG and DTG curves obtained at 20°C·min⁻¹ in nitrogen flow of 20
303 mL·min⁻¹ for TPOMW. The DTG curves show three consecutive degradation steps.
304 Furthermore, the pyrolysis reaction produces a carbonaceous residue that represents the
305 20 wt.% of the raw material. This result is consistent with the values found in the
306 literature for other kinds of biomass (e.g. 21 wt.% for spruce, 30 wt.% for straw and 25-
307 30 wt.% for eucalyptus and poplar) [25].

308

309 Like other biomass sources, the main organic constituents of TPOMW are
310 hemicellulose (38 wt.%), cellulose (21 wt.%) and lignin (46 wt.%) [5]. Hemicellulose

311 pyrolysis mainly happens at 220-315 °C and cellulose thermal degradation ranges from
312 315 to 400 °C, presenting the maximum decomposition rate at 268 °C and 355 °C,
313 respectively. On the other hand, lignin is thermally more stable and its degradation
314 slowly happens under a wide temperature range from 100 to 900 °C, being emphasized
315 in the high temperature region [23, 26]. Thus, the DTG peak at lower temperature is
316 mainly attributed to hemicellulose devolatilization, the second peak mainly corresponds
317 to cellulose decomposition and the last degradation step can involve the degradation of
318 olive oil according to Font and Rey [24]. The degradation of lignin can be contained in
319 the three decomposition steps. Torrefaction was carried out in the range of temperatures
320 from 150 to 300 °C, wherein only one degradation step occurs, representing a total mass
321 loss of 20 wt.%. Accordingly to these results, it is expected that thermal degradation of
322 hemicellulose mainly takes place during torrefaction procedure at tested temperatures,
323 while small degree of cellulose and lignin degradation as well as olive oil
324 decomposition might occurs, which is in agreement with the literature [9, 24, 27].

325

326 3.1.3. FTIR analysis

327 The changes in the chemical structure of TPOMW during torrefaction were analyzed
328 using FTIR spectroscopy. Figure 4 show the spectra of olive oil, TPOMW and t-
329 TPOMW samples. Accordingly, Table 2 reports the assignment of the foremost infrared
330 absorption bands [8, 28].

331

332 The olive oil characteristic bands that appear from 1162 to 1243 cm^{-1} and at 1739 cm^{-1}
333 belong, respectively, to aliphatic ether and alcohol groups and to ester groups, which are
334 also forming part of the chemical structure of hemicellulose and cellulose from

335 TPOMW. As torrefaction temperature rises, it is seen that the intensity of the peaks
336 decreases, which might indicate that the following processes occurs during torrefaction:
337 the degradation of carbohydrates through dehydration and decarboxylation reactions
338 (including the olive oil elimination, as concluded from accelerate solvent extraction
339 results); and the removal of ester group due to deacetylation reactions in hemicellulose.

340

341 Likewise, the peaks located at 723 cm^{-1} and in the range from 1377 to 1461 cm^{-1} are
342 attributed to alkyl C-H groups bending. Hence, the reduction of the intensity of these
343 peaks again indicates a significant thermal degradation of lipids and carbohydrates and
344 the loss of aliphatic chains, which might be related to depolymerization of
345 hemicellulose, since this is the most vulnerable fraction during torrefaction, as seen in
346 the thermogravimetric analysis. Related to this change, it is observed an increase of the
347 peaks ascribed to aromatic skeletal vibrations, which are placed in the range from 1508
348 to 1650 cm^{-1} . Thus, in agreement with the literature [8], this increase supports the
349 assumption that thermal treatment induces the cleavage of ether bond in lignin and the
350 condensation of lignin by linking carbons directly. On the other hand, the loss of
351 carbohydrates also contributes to augment the relative amount of lignin, and therefore,
352 the intensity of the absorption bands corresponding to C=O as the torrefaction
353 temperature increases.

354

355 Thereby, the increase intensity of FTIR signal from aromatic and condensed structure in
356 detriment of aliphatic ones is indicating that the degree of coalification increases during
357 TPOMW torrefaction, being in good agreement with the results presented before.

358

359 *3.1.4. Ash fouling evaluation*

360 One of the major problems associated with biomass combustion is the deposit formation
361 in the convective passes of boilers. These deposits, referred to as slagging and fouling
362 deposits, can drastically reduce heat transfer, cause erosion by channelizing gas flow,
363 and contribute to the corrosion of exposed metal surfaces [29].

364

365 The propensity of fuels for producing slagging and fouling deposits depends on its ash
366 composition. Elements including Si, K, Na, S, Cl, P, Ca, Mg and Fe are involved in
367 reactions leading to ash fouling and slagging. As expected from the literature [5, 29-31],
368 TPOMW-ashes were specially rich in potassium and silicon, which portend potentially
369 severe ash deposition problems at high or moderate combustion temperatures due to two
370 primary sources: the reaction of alkali with silica to form alkali silicates that melt or
371 soften at low temperatures; and the reaction of alkali with sulfur to form alkali sulfates
372 on combustor heat transfer surfaces.

373

374 Although all biomass fuels exhibit fouling behavior, there exist different rates
375 depending on the ash content and composition. Results of the X-ray fluorescence (XRF)
376 analysis are shown in Table 3.

377

378 The alkali index is one of the most significant threshold indicator for fouling and
379 slagging and expresses the quantity of alkali oxide in the fuel per unit of fuel energy (kg
380 alkali·GJ⁻¹). This parameter is calculated by eq. 1, in which HHV is the high heating
381 value of the fuel, Y_f^a is the weight fraction of ash in the fuel and $Y_{K_2O}^a$ and $Y_{Na_2O}^a$ are
382 the weight fractions of K₂O and Na₂O in the ash [29].

383

$$\text{Alkali index} = \frac{Y_f(Y_{K_2O}^a + Y_{Na_2O}^a)}{HHV} \quad [\text{eq. 1}]$$

384

385 Above 0.17 kg alkali GJ^{-1} fouling is probable and above 0.34 kg GJ^{-1} fouling is
386 theoretically certain to occur [29]. According to eq.1, the alkali index for TPOMW is
387 found to be 0.66 kg alkali· GJ^{-1} , which is typical from herbaceous and fruit biomass (e.g.
388 0.50 kg alkali· GJ^{-1} for rice hulls and 0.85 kg alkali· GJ^{-1} for almond shells) and implies
389 that fouling per alkali metals during combustion of TPOMW would occur. Comparing
390 to other fuels, woody biomass has lower alkali index (0.14 kg alkali· GJ^{-1} for willow
391 wood and hybrid poplar) while coal only presents 0.03 kg alkali· GJ^{-1} [29]. Accordingly,
392 fouling tendency of TPOMW could be mitigated through co-firing of TPOMW with
393 appropriate amounts of coal or woody biomass, which present less slagging and fouling
394 problems [29, 30]. A broad combination of fuels have been co-fired in pulverized coal
395 combustion boilers with different proportions of biomass-coal (from 1% to 20%) and
396 experiences has demonstrated that co-firing resulted in less corrosion and ash deposition
397 problems [31]. Then, though co-firing herbaceous biomass tends to be more difficult
398 and costly than others because of its higher inorganic matter content, it would be
399 possible to co-fire such fuels if there were a regulatory incentive to do so [31].

400

401 3.1.5. *Mass and Energy yield*

402 Energy densification via torrefaction allows increasing the heating value through the
403 volatilization of the non-energy compounds while the material energy content is kept as
404 possible [9]. The energy recover (ER) is defined as the energy retained by the solid
405 product, which can be determined by eq.2, in which Y_{solid} represents the solid yield

406 (expressed as %), which is defined as $Y_{\text{solid}} = (m_T/m_0) \cdot 100$, where m_T is the mass of
407 torrefied material produced at temperature T and m_0 the initial mass of dry TPOMW.
408

$$\text{ER} = Y_{\text{solid}} \left(\frac{\text{HHV}_T}{\text{HHV}_0} \right) \cdot 100 \quad [\text{eq. 2}]$$

409
410 Figure 5 shows the Y_{solid} (%) and the ER (%) of t-TPOMW found for each experimental
411 temperature. It can be observed that the ER and the solid yield continually decreases
412 with the increase in the torrefaction temperature, due to the decomposition of some
413 reactive components of the hemicelluloses and the consequent gas products (e.g. carbon
414 monoxide, carbon dioxide, vapor water and acetic acid) volatilization. Solid yield and
415 energy recovery are in the range of approximately 35-98% of the initial weight and 40-
416 99% of the departure energy content. Similar results were reported by Pimchuai et al.
417 [7] for other agricultural residues. However, Ciolkosz and Wallace [9], Prins et al. [13]
418 and Arias et al. [32] reported high solid yields and energy recoveries for torrefied
419 woody biomass, what suggests that the behavior of woody and waste agricultural
420 biomass is different during torrefaction.

421
422 During torrefaction is interesting to increase the heating value by volatilization of non-
423 energetic compounds while trying to keep the energy content of the material treated as
424 possible. Accordingly, Eq. 3 defines the Torrefaction Energy Index (TEI), a parameter
425 that allows, from an energy point of view, determining the temperature at which
426 torrefaction ought to be carried out in order to maximize the heating value while
427 maintaining the maximum energy content as possible from raw wastes. Thus, the higher
428 the TEI parameter, the more torrefaction of biomass will compensate, since a higher

429 value of TEI indicates greater HHV rise or energy densification improvement and lower
430 energy losses. In Eq. 3, ER_T are referred to temperature T.

431

$$TEI = \left(\frac{HHV \text{ rise}}{(100 - ER_T(\%))} \right) \cdot 10 \quad [\text{eq. 3}]$$

432

433 Figure 6 shows the representation of calculated TEI as a function of temperature for
434 TPOMW. As seen in Figure 6, this parameter was also calculated for other agricultural
435 wastes according to the results found by Pimchuai et al. [7]. The curve corresponding to
436 TPOMW present a maximum that indicates the temperature conditions under
437 torrefaction must be carried out accordingly with the criteria assumed, which is found to
438 be 200 °C. This result is consistent with those observed for the other agricultural wastes,
439 since their calculated TEI decrease with increasing torrefaction temperature, which
440 indicates that for this type of materials torrefaction is more energy beneficial at low
441 temperatures due to the energy losses become more important than the HHV rise
442 achieved with increasing temperature. Furthermore, TEI values calculated for rice husks
443 and peanut husks are higher than those obtained for TPOMW as a consequence of the
444 higher HHV rise values and the similar energy losses found for them under the same
445 operation conditions. On the other hand, the opposite behavior is observed for woody
446 biomass, like sawdust: the higher the torrefaction temperature, the higher the TEI,
447 which could be associated to the greater energy recoveries mentioned before as well as
448 the higher HHV rise compared to torrefied agricultural wastes. Therefore, torrefaction
449 of woody biomass could be more energy favorable at 300 °C.

450

451 At this point, it is worth mentioning that if the olive oil that still remains in the torrefied
452 TPOMW when torrefaction is carried out at 200°C might lead to likely problems of
453 odors in future possible combustion applications, such in domestic stoves, from an
454 environmental point of view, the torrefaction temperature would be higher than 250 °C,
455 in order to remove the residual olive oil from the bioenergy feedstocks, even though the
456 energy recovery drops to the 40%. Consequently, if necessary, torrefaction temperature
457 should be based on a compromise solution between the energy and the environmental
458 criteria.

459

460 *3.2. Densification of t-TPOMW*

461 t-TPOMW samples were fragile materials that present higher dust formation capacity
462 than TPOMW, the more the higher was the torrefaction temperature. Furthermore, the
463 energy density ($\text{MJ}\cdot\text{m}^{-3}$) decreases as a result of the porosity generated by removing
464 volatile compounds during torrefaction. Therefore, it is necessary to volumetrically
465 densify the t-TPOMW.

466

467 Some briquetting tests were carried out using t-TPOMW-200, t-TPOMW-250 and t-
468 TPOMW-300 in order to analyze the viability of the densification process. It was found
469 that for all the three analyzed materials it is possible to produce briquettes having a bulk
470 density of $1\text{ kg}\cdot\text{cm}^{-3}$ and considerable mechanical strength at temperature of 200 °C and
471 compression pressure of 17 MPa due to during compression at high temperatures, the
472 protein and starch plasticizes and the lignin softens above 140 °C [17], which improves
473 the particles binding and, consequently, assists in increasing the briquettes strength. In
474 addition, around a 4% of the residual olive oil contained in t-TPOMW-200 and t-

475 TPOMW-250 was also removed during stress application, with the over mentioned
476 benefits in future purposes.

477

478 Table 4 shows the evolution of the energy density ($\text{MJ}\cdot\text{m}^{-3}$) when applying the
479 torrefaction process to TPOMW at 200 °C, 250°C and 300°C and the briquetting method
480 to torrefied TPOMW at 200 °C and 17 MPa. It is seen that the technology of
481 torrefaction combined with densification is able to increase the energy density of
482 TPOMW by approximately 232%, 237% and 242% for t-TPOMW-200, t-TPOMW-250
483 and t-TPOMW-300 briquettes, respectively, so that, briquetting is a feasible way to
484 densify t-TPOMW feedstock. Additionally, Table 4 also shows the energy density of
485 woody biomass, lignite and anthracite for comparison [32]. It is seen that energy density
486 of densified torrefied materials are intermediate to low rank and high rank coals.

487

488 Al-Widyan et al. [33] evaluated the physical quality of olive cake briquettes made by
489 compressing in a hydraulic press under different levels of stress, moisture content and
490 dwell time. These authors indicated that for samples with low moisture content the most
491 significant parameter on briquette quality was the level of stress and found that a stress
492 level closed to 34 MPa produced the best results, which may be considered as optimal
493 stress. By comparing this pressure with that used for t-TPOMW briquetting, it can be
494 seen that the stress level required to densify olive cake duplicates the stress level used to
495 densify t-TPOMW. Hence, although more research is needed in order to optimize both
496 the densification system and the variables that controlled the process, torrefaction is also
497 beneficial to reduce the specific energy consumption during densification.

498

499 **4. Conclusion**

500 Results have demonstrated that a profitable bioenergy feedstock can be produced via
501 torrefaction of TPOMW, which implies a feasible elimination of this agricultural waste.
502 An increase of torrefaction temperature results in a linear decrease of oxygen content
503 and higher HHV, finding that, from an energy point of view, the temperature for
504 TPOMW torrefaction lies nearby to 200 °C. However, the TPOMW torrefied at this
505 temperature still contain a 24 wt.% of olive oil. Then, in those energy applications
506 where odors posed problems, torrefaction temperature should be based on a
507 compromise solution between the energy and the environmental criteria. Besides,
508 enhanced bulk density TPOMW briquettes with excellent mechanical strength can be
509 produced using a hydraulic piston press at mild conditions. Summarizing, torrefaction
510 combined with briquetting emerged as a promising option for treating two-phase olive
511 mill waste and produce bioenergy feedstock.

512

513 **5. Acknowledgements**

514 This research was supported by the Spanish Ministry of Economy and Competitiveness
515 (MINECO) and the European Regional Development Fund (FEDER) (IPT-2012-0565-
516 310000).

517

518 **6. References**

519 [1] International Energy Agency. World Energy Outlook 2011. Available at
520 <<http://www.iea.org/publications/freepublications/publication/name,37085,en.html>>;
521 November 2013.

522

- 523 [2] Schmidhube J. Impact of an increased biomass use on agricultural markets, prices
524 and food security: A longer-term perspective. Available at
525 <[http://www.globalbioenergy.org/uploads/media/0704__Schmidhuber_-
526 _Impact_of_an_increased_biomass_use_on_agricultural_markets__prices_and_food_se
527 curity.pdf](http://www.globalbioenergy.org/uploads/media/0704__Schmidhuber_-_Impact_of_an_increased_biomass_use_on_agricultural_markets__prices_and_food_security.pdf)>; November 2013.
528
- 529 [3] International Olive Council. The world market in figures. *Olivae* 2012; 117: 28-34.
530
- 531 [4] Olive Oil Agency of Spanish Ministry of Agriculture, Fishing and Food. Report on
532 the olive oil and table olives (Campain 2012-2013) 2013. Available at
533 <[http://www.faeca.es/files/Documentacion/Aceite%20y%20aceituna/Informe_AAO_ju
534 n_2013.pdf](http://www.faeca.es/files/Documentacion/Aceite%20y%20aceituna/Informe_AAO_jun_2013.pdf)>; November 2013.
535
- 536 [5] Albuquerque JA, González J, García D, Cegarra J. Agrochemical characterisation
537 of "alperujo", a solid by-product of the two-phase centrifugation method for olive oil
538 extraction. *Bioresour Technol* 2004; 91: 195-200.
539
- 540 [6] Roig A, Cayuela ML, Sánchez-Monedero MA. An overview on olive mill wastes
541 and their valorisation methods. *Waste Manage* 2006; 26: 960-9.
542
- 543 [7] Pimchuai A, Dutta A, Basu P. Torrefaction of agriculture residue to enhance
544 combustible properties. *Energy Fuels* 2010; 24: 4638-45.
545

546 [8] Park J, Meng J, Lim KH, Rojas OJ, Park S. Transformation of lignocellulosic
547 biomass during torrefaction. *J Anal Appl Pyrolysis* 2013; 100: 199-206.
548

549 [9] Ciolkosz D, Wallace R. A review of torrefaction for bioenergy feedstock production.
550 *Biofuel Bioprod Biorefining* 2011; 5: 317-29.
551

552 [10] Wannapeera J, Worasuwannarak N. Upgrading of woody biomass by torrefaction
553 under pressure. *J Anal Appl Pyrolysis* 2012; 96: 173-80.
554

555 [11] Duncan A, Pollard A, Fellouah H. Torrefied, spherical biomass pellets through the
556 use of experimental design. *Appl Energy* 2013; 101: 237-43.
557

558 [12] Chen W, Hsu H, Lu K, Lee W, Lin T. Thermal pretreatment of wood (Lauan)
559 block by torrefaction and its influence on the properties of the biomass. *Energy* 2011;
560 36: 3012-21.
561

562 [13] Prins MJ, Ptasinski KJ, Janssen FJJG. Torrefaction of wood: part 1. Weight loss
563 kinetics. *J Anal Appl Pyrolysis* 2006; 77(1):28-34.
564

565 [14] Prins MJ, Ptasinski KJ, Janssen FJJG. Torrefaction of wood: part 2. Weight loss
566 kinetics. *J Anal Appl Pyrolysis* 2006; 77(1):35-40.
567

568 [15] Bergman PCA, Boersma AR, Zwart RWR, Kiel JHA. Torrefaction for biomass co-
569 firing in existing coal-fired power stations "biocoal". Report ECN-C.05-013. Petten,
570 The Netherlands: ECN; 2005.
571

572 [16] Rousset P, Macedo L, Commandré JM, Moreira A. Biomass torrefaction under
573 different oxygen concentrations and its effect on the solid by-product. J Appl Anal
574 Pyrolysis 2012; 96: 86-91.
575

576 [17] Tumuluru JS, Wright CT, Hess JR, Kenney KL. A review of biomass densification
577 systems to develop uniform feedstock commodities for bioenergy application. Biofuel
578 Bioprod Biorefining 2011; 5: 683-707.
579

580 [18] Uemura Y, Omar WN, Tsutsui T, Yusup SB. Torrefaction of oil palm wastes. Fuel
581 2001;90(8):2585-91.
582

583 [19] Arcate JR. Torrefied wood, an enhanced wood fuel. Bioenergy; 2002. Boise;Idaho;
584 September 22-26;2002.
585

586 [20] Felfi FF, Luengo CA, Suarez JA, Beaton PA. Wood briquette torrefaction. Energy
587 Sustain Develop 2005;9(3):19-22.
588

589 [21] Indian Institute of Science. Project completion on torrefaction of
590 bamboo,<http://cgpl.iisc.ernet.in>; 2006.
591

- 592 [22] NETL-National Energy Technology Laboratory. Cost and performance baseline for
593 fossil energy plants. Volume 3b: Low rank coal to electricity. Combustion cases. 2011;
594 DOE/NETL - 2011/1463.
595
- 596 [23] Özveren U, Özdoğan ZS. Investigation of the slow pyrolysis kinetics of olive oil
597 pomace using thermo-gravimetric analysis coupled with mass spectrometry. Biomass
598 Bioenergy 2013, <http://dx.doi.org/10.1016/j.biombioe.2013.08.011>.
599
- 600 [24] Font R, Rey MD. Kinetics of olive oil pyrolysis. J Anal Appl Pyrolysis 2013;
601 103:181-88.
602
- 603 [25] Van de Velden M, Baeyens J, Brems A, Janssens B, Dewil R. Fundamentals,
604 kinetics and endothermicity of the biomass pyrolysis reaction. Renew Energy 2010; 35:
605 232-42.
606
- 607 [26] Yang H, Yan R, Chen H, Lee DH, Zheng C. Characteristics of hemicellulose,
608 cellulose and lignin pyrolysis. Fuel 2007; 86: 1781-8.
609
- 610 [27] Chen W-, Kuo P-. Isothermal torrefaction kinetics of hemicellulose, cellulose,
611 lignin and xylan using thermogravimetric analysis. Energy 2011; 36: 6451-60.
612
- 613 [28] Droussi Z, D'orazio V, Provenzano MR, Hafidi M, Ouattmane A. Study of the
614 biodegradation and transformation of olive-mill residues during composting using FTIR
615 spectroscopy and differential scanning calorimetry. J Hazard Mater 2009; 164: 1281-5.

616

617 [29] Jenkins BM, Baxter LL, Miles Jr. TR, Miles TR. Combustion properties of
618 biomass. *Fuel Proces Technol* 1998; 54: 17-46.

619

620 [30] Kalembkiewicz J, Chmielarz U. Ashes from co-combustion of coal and biomass:
621 New industrial wastes. *Resour Conserv Recycl* 2012; 69: 109-21.

622

623 [31] Al-Mansour F, Zuwala J. An evaluation of biomass co-firing in Europe. *Biomass*
624 *Bioenergy* 2010; 34: 620-9.

625

626 [32] Arias B, Pedida C, Feroso J, Plaza MG, Rubiera F, Pis JJ. Influence of
627 torrefaction on the grindability and reactivity of woody biomass. *Fuel Process. Technol.*
628 2008; 89: 169–175.

629

630 [33] Canalís P, Royo J, Sebastián F, Pascual J, Tapia R. La co-combustión: una
631 alternativa para la utilización de la biomasa residual. *InfoPower* 2003; 58: 11-4.

632

633 [34] Al-Widyan MI, Al-Jalil HF, Abu-Zreig MM, Abu-Hamdeh NH. Physical durability
634 and stability of olive cake briquettes. *Can Biosyst Eng* 2002; 44: 3.41,3.46.

635

636

637

638

639

640

641 **Tables**

642

643 Table 1. Ultimate analysis (% dry basis), ash content (wt.%), olive oil content (wt.%)
 644 and high heating values (HHV, MJ·kg⁻¹) of TPOMW and t-TPOMW samples and HHV
 645 rise (%) of t-TPOMW samples.

646

Values (% dry basis)	TPOMW	t-TPOMW-150°C	t-TPOMW-200°C	t-TPOMW-250°C	t-TPOMW-300°C
<i>Ultimate Analysis</i>					
C	56.1	59.9	66.3	67.2	67.7
H	7.4	8.0	8.9	8.0	4.1
N	0.8	1.1	1.7	1.6	1.6
O	29.9	25.0	16.2	14.0	10.1
S	<0.1	<0.1	<0.1	<0.1	<0.1
Ash content (wt.% d.b.)	5.5	5.6	6.5	8.7	15.7
Olive oil content (wt.%d.b.)	26.0	25.0	24.1	19.9	0.1
HHV (MJ·kg ⁻¹)	26.4	26.5	28.7	29.4	30.0
HHV rise (%)	-	0.4	8.6	11.0	13.4

647

648

649

650

651

652

653

654

655

656

657 Table 2. Main functional groups of TPOMW and t-TPOMW on FTIR spectra.

658

Wave number (cm ⁻¹)	Range (cm ⁻¹)	Functional groups	Mode of vibration
673	640-701	O-H	bending (out of plane)
723	-	C-C -(CH ₂) _n - -HC=CH- (cis)	bending (out of plane) rocking bending (out of plane)
1018	1006-1043	-C-O	stretching
1162	1147-1211	-C-O	stretching
1243	1211-1290	-C-O	stretching
1377	1371-1382	-C-H (CH ₃)	bending symmetric
1446	1446-1486	-C-H (CH ₃)	bending assymmetric
1461	1446-1486	-C-H (CH ₂)	bending scissoring
1508	-	C=C (aromatic)	stretching
1650	1640-1651	C=C (aromatic) C=O (amine groups, amine II band)	skeletal vibrations stretching
1739	1677-1795	-C=O (ester)	stretching

659

660

661 Table 3. XRF analysis of TPOMW-ashes (expressed as percentage of oxides by

662 weight).

663

Oxide constituent	K ₂ O	SiO ₂	MgO	P ₂ O ₅	CaO	Al ₂ O ₃	Fe ₂ O ₃	SO ₃	TiO ₂
Ash basis (%)	31.9	27.8	18.4	6.8	5.5	5.1	1.6	1.1	0.2

664

665

666

667

668 Tabla 4. Energy density of TPOMW, t-TPOMW-200 and t-TPOMW-200-briquette.

669

Energy feedstock	Energy Density (MJ·m⁻³)
TPOMW	12397
t-TPOMW-200	11343
t-TPOMW-250	10385
t-TPOMW-300	9366
t-TPOMW-200 briquette	28712
t-TPOMW-250 briquette	29410
t-TPOMW-300 briquette	29994
<i>For comparing*</i>	
Forest biomass	12040
Low rank coal	16300
High rank coal	39000

*Data from Canalí et al., 2003.

670

671

672 **Figures**

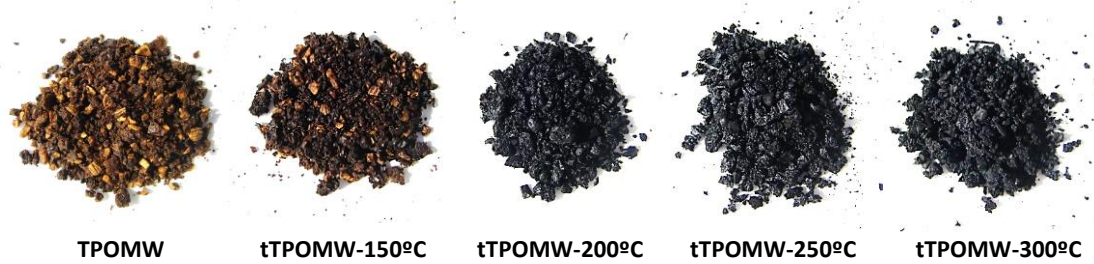
673

674 Figure 1. Pictures of the torrefied materials derived at various temperatures.

675

676

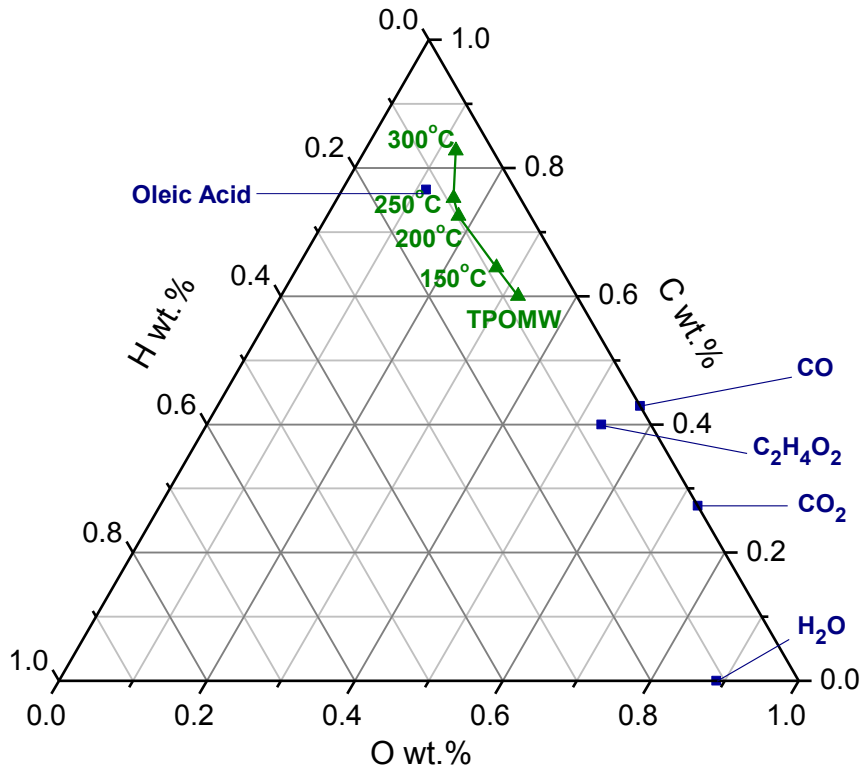
677



678

679

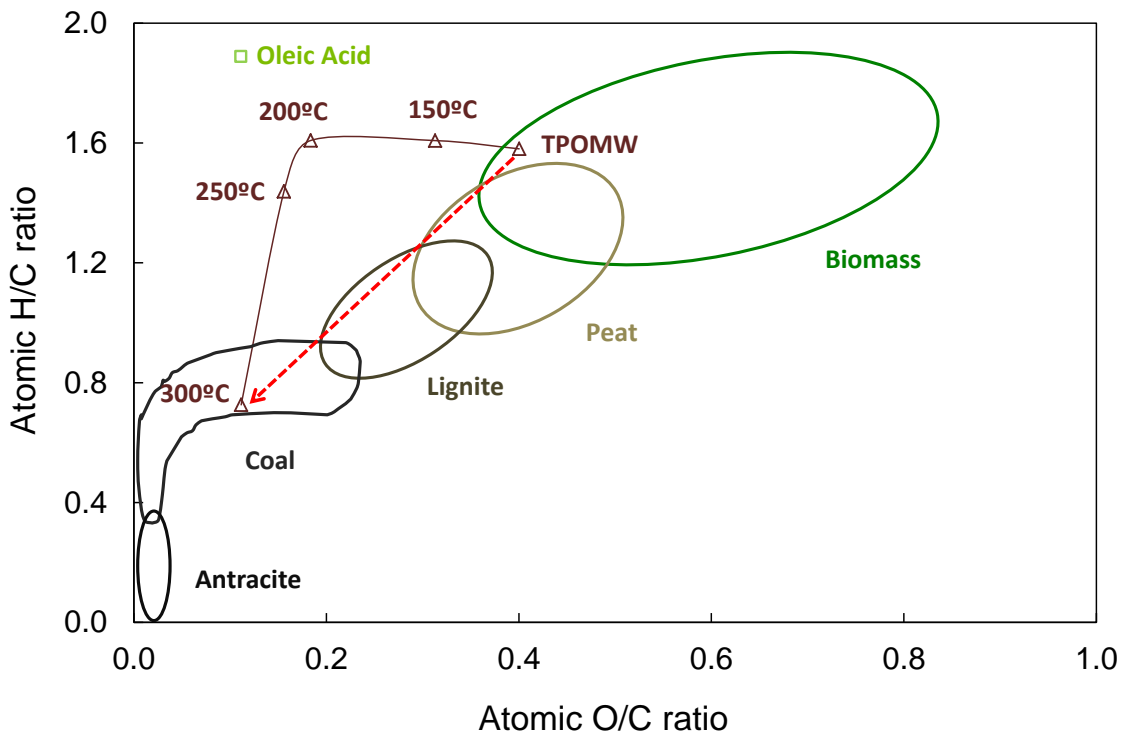
680 Figure 2. A) Effect of torrefaction temperature illustrated in a CHO diagram.



681

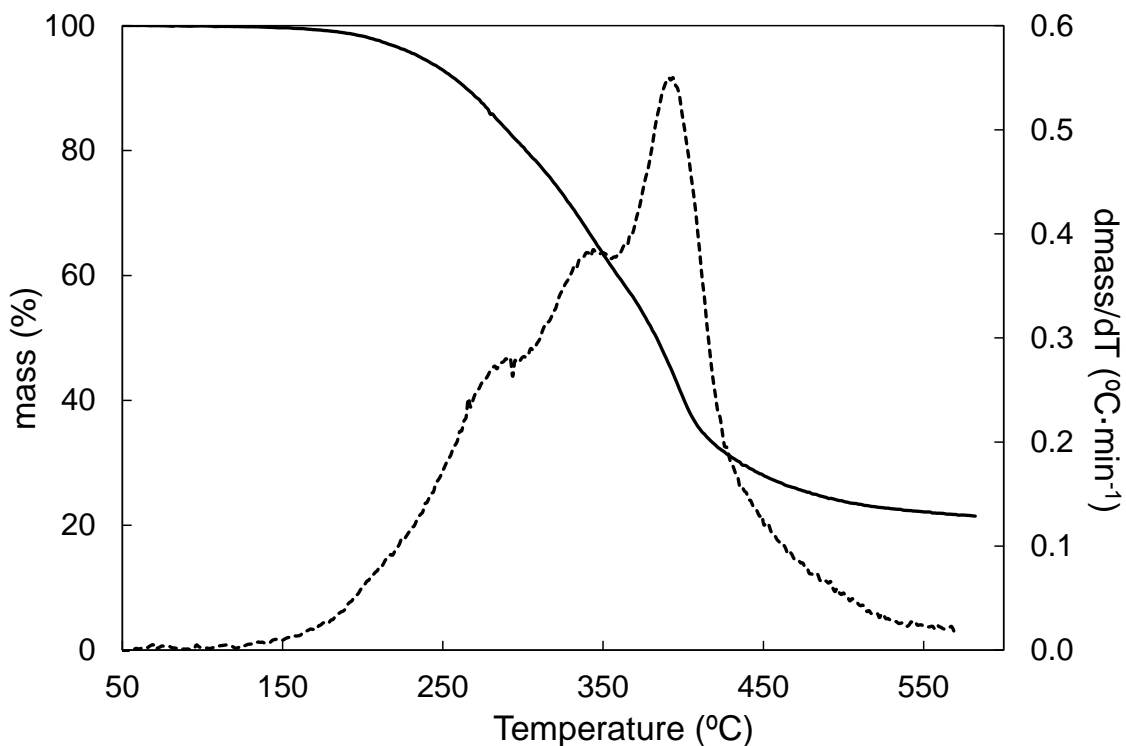
682 Figure 2. B) Compositional differences among TPOMW and t-TPOMW in van

683 Krevelen diagram.

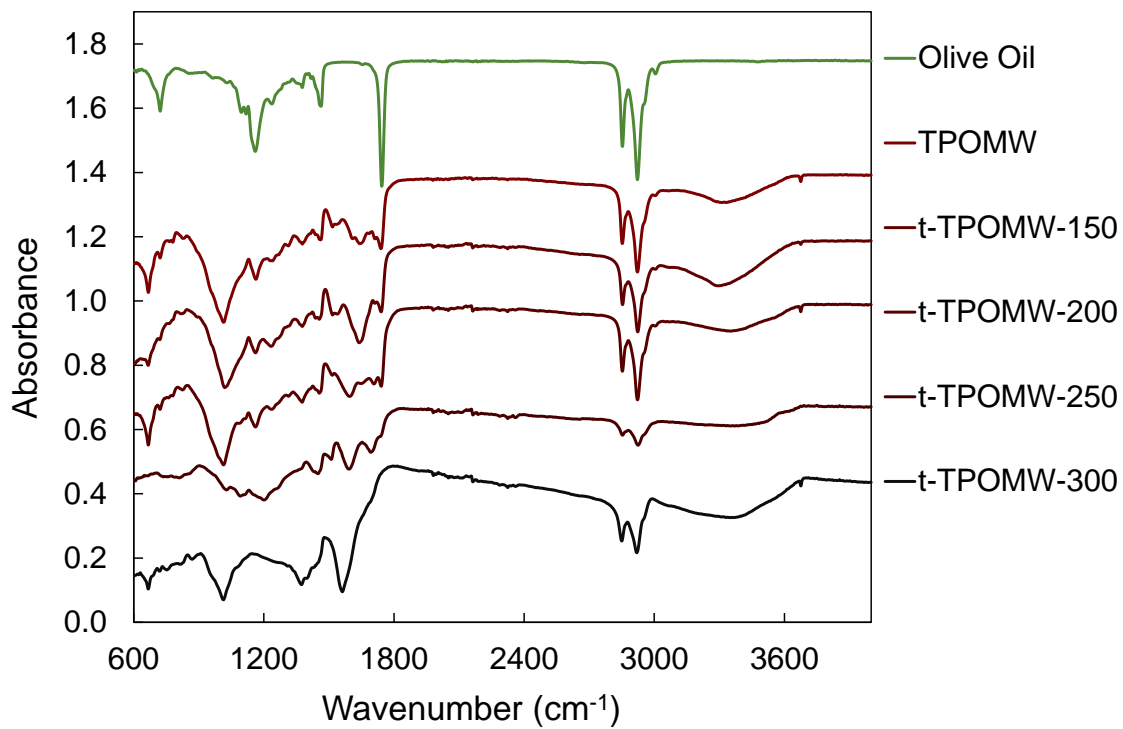


684

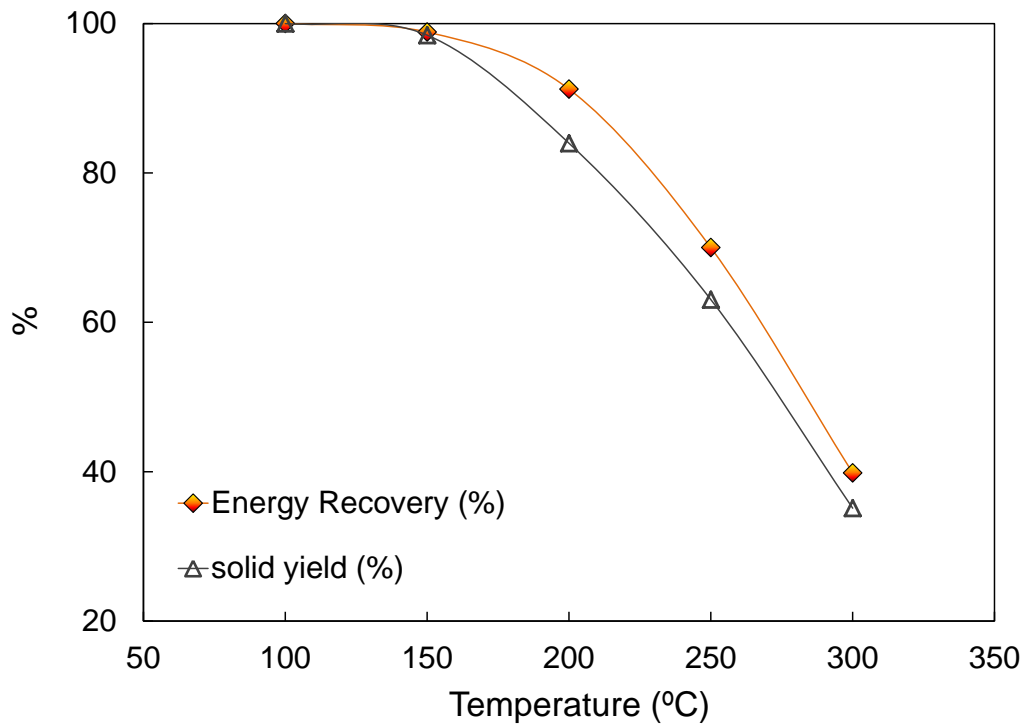
685 Figure 3. TG and DTG curves for TPOMW at $20^{\circ}\text{C}\cdot\text{min}^{-1}$ under nitrogen atmosphere.
686
687



688
689
690
691 Figura 4. FTIR spectra of olive oil, raw TPOMW and t-TPOMW.



693 Figure 5. Energy recovery (%) and solid yield (%) for t-TPOMW.

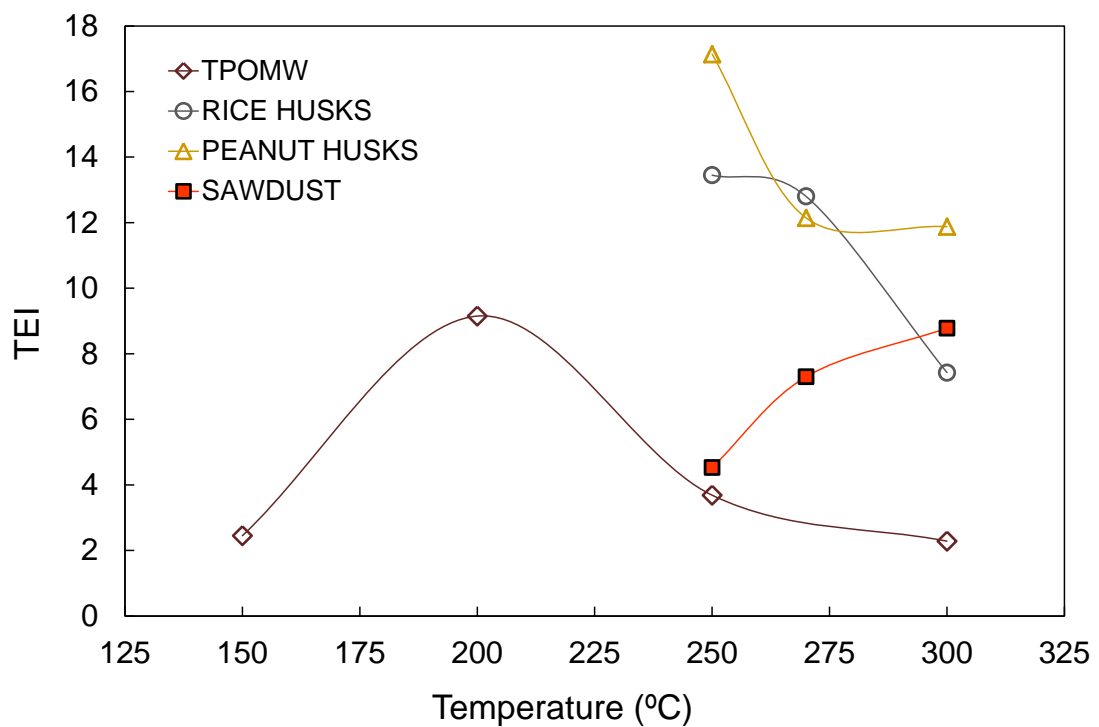


694

695

696 Figure 6. Calculated Torrefaction Energy Index (TEI) as a function of temperature for

697 TPOMW and other agricultural wastes from the literature [7].



698